

[2] Calculation of angular and spectral selectivity for full-parallax holographic stereograms



D.S. Lushnikov¹, A.Y. Zherdev¹, V.V. Markin¹, S.B. Odinokov¹, A.V. Smirnov²

¹ Bauman Moscow State Technical University, Moscow, Russia,

² JSC "RPC "Krypten", Dubna, Russia

Abstract

In this paper, dependencies of the angular and spectral selectivity on the incidence angle of the reference beam in a scheme for obtaining reflection and transmission holograms are obtained and analyzed. It is shown that for obtaining color holographic stereograms a scheme for obtaining transmission holograms is more suitable. While the angular selectivity of reflection and transmission color holograms is the same, the spectral selectivity of the reflection hologram is much higher at all wavelengths of recording. A method and equipment for one-step digital recording of color full-parallax holographic stereograms with rasterless image are developed. Samples of color full-parallax security holographic stereograms with a "flip-flop" effect in the image were obtained. The quality of the reconstructed image verifies high spectral selectivity for this type of holograms.

Keywords: SECURITY HOLOGRAMS, COLOR HOLOGRAMS; MULTIPLEX HOLOGRAMS; HOLOGRAPHIC STEREOGRAMS

Citation: LUSHNIKOV DS, ZHERDEV AY, MARKIN VV, ODINOKOV SB, SMIRNOV SV

CALCULATION OF ANGULAR AND SPECTRAL SELECTIVITY FOR FULL-PARALLAX HOLOGRAPHIC STEREOGRAMS.

COMPUTER OPTICS, 2016; 40(6): 802–809.

DOI: 10.18287/2412-6179-2016-40-6-802-809.

Introduction

Holographic stereograms (HS) is a hologram type that reconstructs a package of superimposed two-dimensional object images, each being observed from particular direction of view. During the observation of given multiview hologram, viewer sees two different images that create a stereo effect. Viewer displacement in the field of view formation leads to the interchange image pair, and object rotation. In case of one-parallax holography, stereo effect appears just in a horizontal plane. Full-parallax holograms can create a stereo effect in both directions: horizontal and vertical.

1. Angular and spectral selectivity analysis

Main parameters of both hologram types (reflective and transparent) includes angular δ_α and spectral δ_λ selectivity. When recording holograms with a non-shrinking photomaterial, the first one (δ_α) defines angular width of diffraction efficiency outline η , varying reconstruction beam incident angle α from incident angle α_0 while recording. The second one

(δ_λ) defines spectral width of diffraction efficiency outline η varying reconstruction beam wavelength λ from wavelength λ_0 while recording the hologram. The following estimation constitutes approximate values of angular and spectral selectivity. A recording photosensitive medium for that purpose is 10 μm thick (for example, silver halide photosensitive plates PFG-03C produced by «Slavich» factory, Russia). Parameter values are defined at the level of 0,5.

For phase reflective hologram the value of δ_α can be specified [1, 2] as

$$\delta_\alpha = \frac{\xi_r}{\frac{2\pi n}{\lambda_0} T \cos \Theta_0},$$

where ξ_r – a parameter, proportional to angular deviation δ_α from Bragg angle selecting with Fig. 1 curves of relative diffraction efficiency η/η_0 (η and η_0 – diffraction efficiency corresponding to deviation from Bragg angle by the value of δ and to same zero deviation); n – average refractive index of the recording medium; T – a thickness of the recording medium; Θ_0 – Bragg angle in the recording medium.

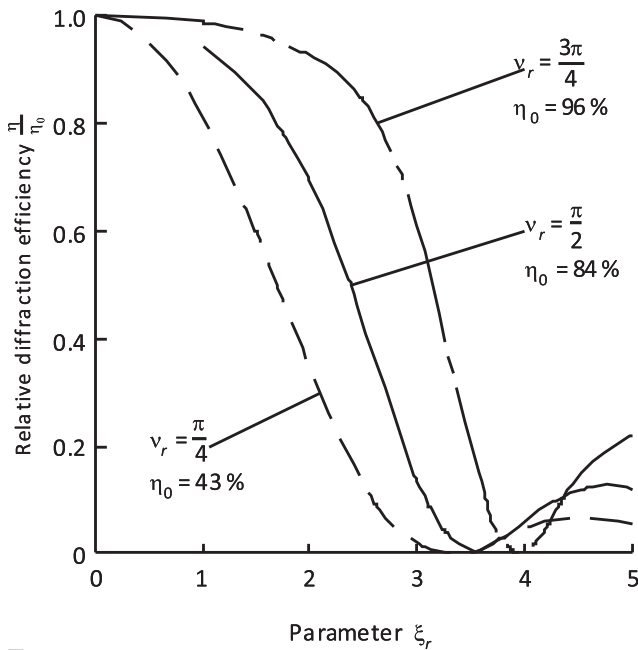


Fig. 1. Relative diffraction efficiency curves depending on ν_r parameter for reflective hologram

Angular selectivity in air is determined as

$$\delta_{\alpha}^{\text{air}} = n\delta_{\alpha}. \tag{1}$$

In addition, spectral selectivity δ_{λ} connects with angular selectivity δ_{α} [1, 2] by the formula

$$\delta_{\lambda} = \frac{\delta_{\alpha}\lambda_0}{\text{tg } \Theta_0}. \tag{2}$$

Curves for $\eta/\eta_0(\xi_r)$ in Fig. 1 are performed for different values of the ν_r parameter proportional to modulation amplitude of the refractive index, resulting in response to exposure and hologram processing. It also defines reconstructing-reconstructed relationship of the radiation.

Parameter estimation is made using layers recording medium PFG-03C with standard thickness $T = 10 \mu\text{m}$, $n = 1.52$ for three recording wavelengths: $\lambda_{01} = 440 \text{ nm}$, $\lambda_{02} = 532 \text{ nm}$ and $\lambda_{03} = 660 \text{ nm}$ generated by laser Geola RGB- β -1064 for color holography. With the value $\nu_r = \pi/4$, providing $\eta_0 = 43\%$ and setting $\eta/\eta_0 = 0.5$ as level limit, the value $\xi_r = 1.7$ is graphically defined. In counter-directional scheme to record the reflective holograms, given that the incident angle of object beam is $\alpha_0 = 0^\circ$ and the angle of reference beam is β_0 , the value Θ_0 is written as

$$\Theta_0 = 90^\circ - \frac{\arcsin \frac{\sin \beta_0}{n}}{2}.$$

For phase transparent hologram the value of δ_{α} can be determined [2] as

$$\delta_{\alpha} = \frac{\xi_t}{\frac{2\pi n}{\lambda_0} T \sin \Theta_0}.$$

The presentational calculation is performed with pre-definite T , n , λ_0 . The value ξ_t is defined with the same condition of the ν parameter as for the reflective hologram conforming to graphics in Fig. 2. For $\nu = \pi/4$ with providing $\eta/\eta_0 = 0.5$ it is $\xi_t = 1.4$.

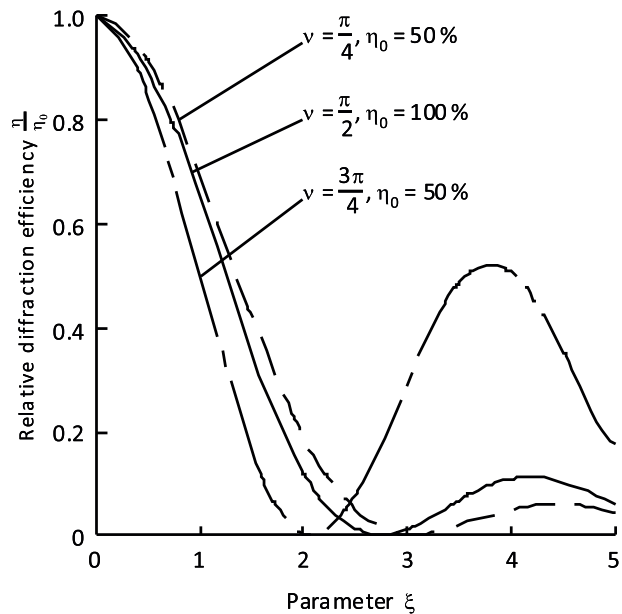


Fig. 2. Relative diffraction efficiency curves depending on ν_r parameter for transparent hologram

$$\Theta_0 = 90^\circ - \frac{\arcsin \frac{\sin \beta_0}{n}}{2}.$$

In this case, angular selectivity in air $\delta_{\alpha}^{\text{air}}$ and spectral selectivity δ_{λ} are defined in accordance to equations (1) and (2).

Tables 1–4 and figures 3–6 present the calculation results for angular δ_{α} and spectral δ_{λ} selectivity values conforming to reflective and transparent holograms for aforementioned wavelengths. The calculation were carried out for the incident angles of reference beam in range $30\text{--}85^\circ$. The whole calculation were performed for attitudes of an equiphase surface either in parallel to a hologram plane (for reflective holograms) or normal thereto (for transparent holograms). However, when beams with complex wave fronts interfere, given surfaces could have arbitrarily orientations, so it becomes necessary to use more complicated computations as described in [3].

Table 1. Angular selectivity $\delta\alpha$ depending on reference beam incident angle during the recording (reflective hologram)

Reference beam incident angle $\beta_0, ^\circ$	Angular selectivity $\delta\alpha, ^\circ$		
	$\lambda_1 = 440 \text{ nm}$	$\lambda_2 = 532 \text{ nm}$	$\lambda_3 = 660 \text{ nm}$
30	8.178	9.888	12.267
35	7.095	8.579	10.643
40	6.299	7.616	9.448
45	5.694	6.885	8.541
50	5.226	6.319	7.839
55	5.226	5.875	7.289
60	4.570	5.526	6.856
65	4.344	5.253	6.517
70	4.171	5.043	6.256
75	4.041	4.886	6.062
80	3.952	4.779	5.928
85	3.900	4.715	5.850

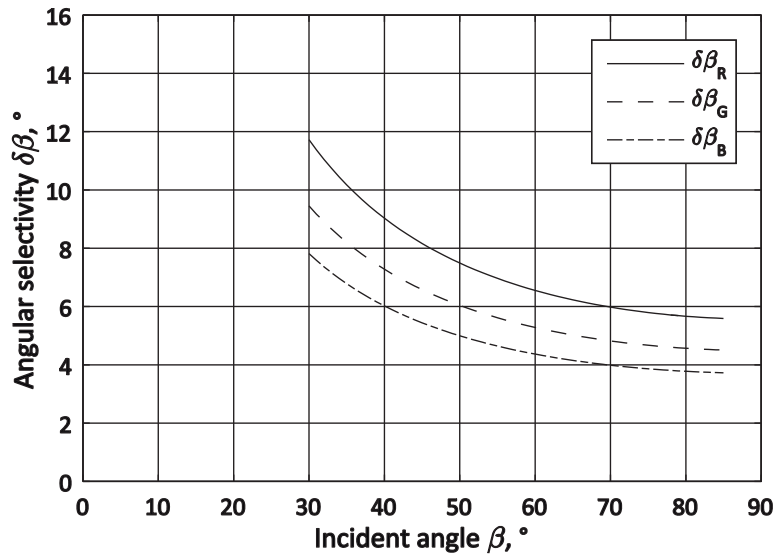


Fig. 3. Reference beam incident angle vs angular selectivity curves for reflective holograms

Table 2. Spectral selectivity $\delta\lambda$ depending on reference beam incident angle during the recording (reflective hologram)

Reference beam incident angle $\beta_0, ^\circ$	Spectral selectivity $\delta\lambda, \text{ nm}$		
	$\lambda_1 = 440 \text{ nm}$	$\lambda_2 = 532 \text{ nm}$	$\lambda_3 = 660 \text{ nm}$
30	6.990	10.219	15.728
35	7.023	10.267	15.802
40	7.060	10.321	15.885
45	7.099	10.378	15.973
50	7.140	10.438	16.065
55	7.181	10.498	16.157
60	7.221	10.557	16.248
65	7.259	10.613	16.334
70	7.293	10.662	16.410
75	7.322	10.704	16.474
80	7.344	10.736	16.523
85	7.357	10.755	16.553

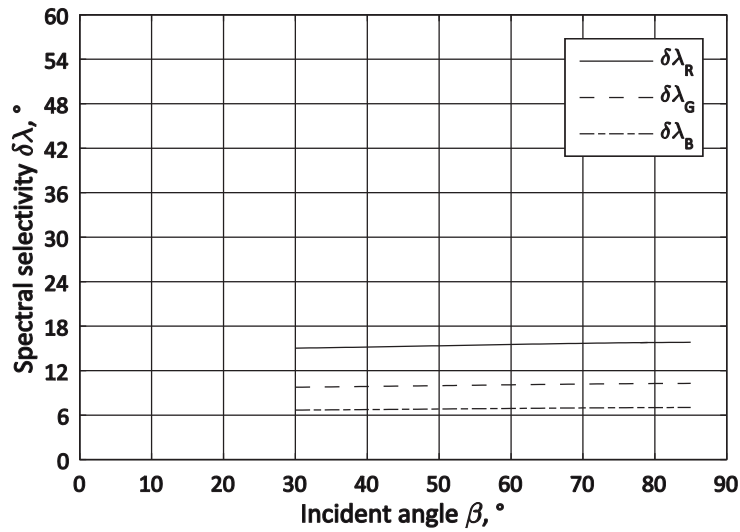


Fig. 4. Reference beam incident angle vs spectral selectivity curves for reflective holograms

Table 3. Angular selectivity $\delta\alpha$ depending on reference beam incident angle during the recording (transparent hologram)

Reference beam incident angle $\beta_0, ^\circ$	Angular selectivity $\delta\alpha, ^\circ$		
	$\lambda_1 = 440 \text{ nm}$	$\lambda_1 = 440 \text{ nm}$	$\lambda_1 = 440 \text{ nm}$
30	6.735	8.143	10.102
35	5.843	7.065	8.765
40	5.187	6.272	7.781
45	4.689	5.670	7.034
50	4.304	5.204	6.456
55	4.002	4.838	6.002
60	3.764	4.551	5.646
65	3.578	4.326	5.367
70	3.435	4.153	5.152
75	3.328	4.024	4.992
80	3.255	3.935	4.882
85	3.212	3.883	4.818

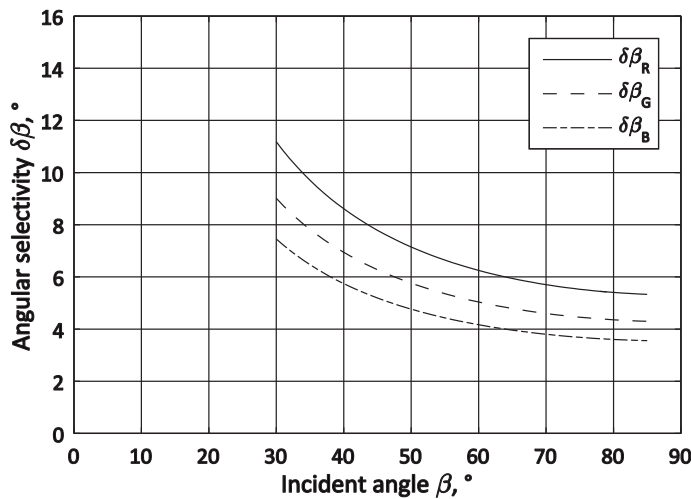


Fig. 5. Reference beam incident angle vs angular selectivity curves for transparent holograms

Table 4. Spectral selectivity dI depending on reference beam incident angle during the recording (transparent hologram)

Reference beam incident angle $\beta_0, ^\circ$	Spectral selectivity $\delta_\lambda, \text{ nm}$		
	$\lambda_1 = 440 \text{ nm}$	$\lambda_2 = 532 \text{ nm}$	$\lambda_3 = 660 \text{ nm}$
30	201.124	294.023	452.528
35	150.684	220.285	452.528
40	118.128	172.692	265.789
45	96.009	140.355	216.019
50	80.409	117.550	180.920
55	69.115	101.040	155.510
60	60.805	88.891	136.811
65	54.653	79.897	122.968
70	50.130	73.285	112.792
75	46.891	68.551	105.506
80	44.714	65.368	100.607
85	43.459	63.532	97.782

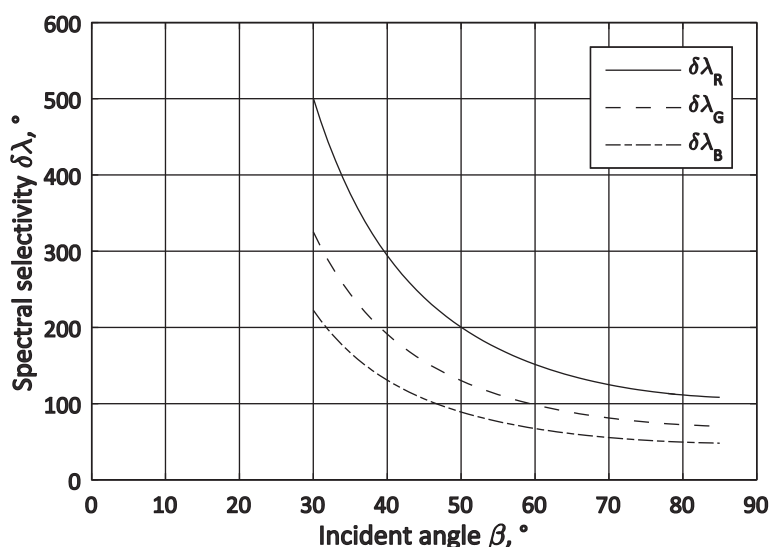


Fig. 6. Reference beam incident angle vs spectral selectivity curves for transparent holograms

Represented tables show that spectral selectivity of reflective hologram is higher, providing good-quality reconstruction for all of the color components. It also does not have much depend on the incident angle of reference beam for each one of color component. Conversely, spectral selectivity of the transparent hologram for the small incident angles of reference beam is very low. That fact prohibits receiving qualitative reconstruction of all color component.

With increase of the incident angle, when recording the transparent hologram, the spectral selectivity grows, but has a quite small value even if the incident angle of reference beam is extremely high. These points to the fact that it is impossible to achieve good-quality reconstruction of the color image from the transparent hologram commensurate with the same from the reflective hologram. Transparent hologram reconstructs colors much less

«clean» than reflective one. Furthermore, angular selectivity of the transparent and reflective hologram are quite similar. That leads to the conclusion that both hologram types have similar «blurring» in the reconstructed image when using not point light source.

2. Apparatus for recording holographic stereograms

Present-day high efficiency systems of HS obtaining are digital, in an objective branch using a liquid crystalline (LC) space-time light modulators (SLM) with computer serial image output. One-step raster systems are widespread in holography to record stereograms. In raster holographic systems, so called holographic printer, the hologram and its object image are formed as one-dimensional raster when recording one-parallax stereograms

[4, 5] or two-dimensional raster when recording full-parallax stereograms [6]. In that kind of system every single raster element in the hologram provides the reconstruction to the whole set of views for the corresponding element of the object image. The obtaining of such an element is in the registration in the photosensitive medium of the holographic field from interference of reference and object beams. In that case, object beam carries information, constituting space-division sub-beams about all of the angles of the recording image element. Accordingly, image outputting to LC SLM in object beam cannot be displayed as one given image, but rather complex image generated by a specific algorithm. This requires additional pre-processing on images and complicates the equipment when recording stereograms.

In this type equipment, the conspicuous requirement is to minimize raster element in the hologram to the size of resolution limit when observing the hologram. With a normal eye resolution as one arc minute when observing the hologram from a distance of 400 mm, the size of the raster element should not exceed 0.1 mm. To obtain such small dimensions for raster element only with square or slit aperture, placed in front of the recording medium, is problematic and can be achieved by complicating the optical scheme of the apparatus. It is also necessary to be aware of quality deterioration in the reconstructed image due to radiation scattering on raster structure of the hologram, as well as raster pattern of the image does not allow to include some fine-structure security elements in there, for example, microtext or Fresnel elements.

Full-color HS recording requires laser system that generates radiation of red, green, and blue wavelengths. The recording systems for raster HS establish either multiplex recording of the raster element [6, 7] or parallel recording of the raster [8], both using different wavelengths. The alternate design of multiplex recording apparatus, which requires combining three beams from different wavelengths in one channel, is accompanied by increase in requirements for the optical system. As a result, it gets more complicated, as well as diffraction efficiency of HS decrease due to multiplexing. The alternate design of a parallel recording apparatus is accompanied by its cumbersomeness.

3. Set up scheme for recording holographic stereograms

All the aforementioned shortcomings led to the creation of one fundamentally different system for HS recording, especially convenient in the recording of security stereograms. This case is distinguished with no need to obtain large holograms, but the enhanced image quality to enable the inclusion of small-structure security elements into the image, as noted above. The developed optical scheme, implementing a single-stage digital recording for color holograms with the formation of rasterless image in the hologram plane, is shown at Fig. 7 as in a top view (in the horizontal projection). An alternative for the recording of reflective HS is represented here.

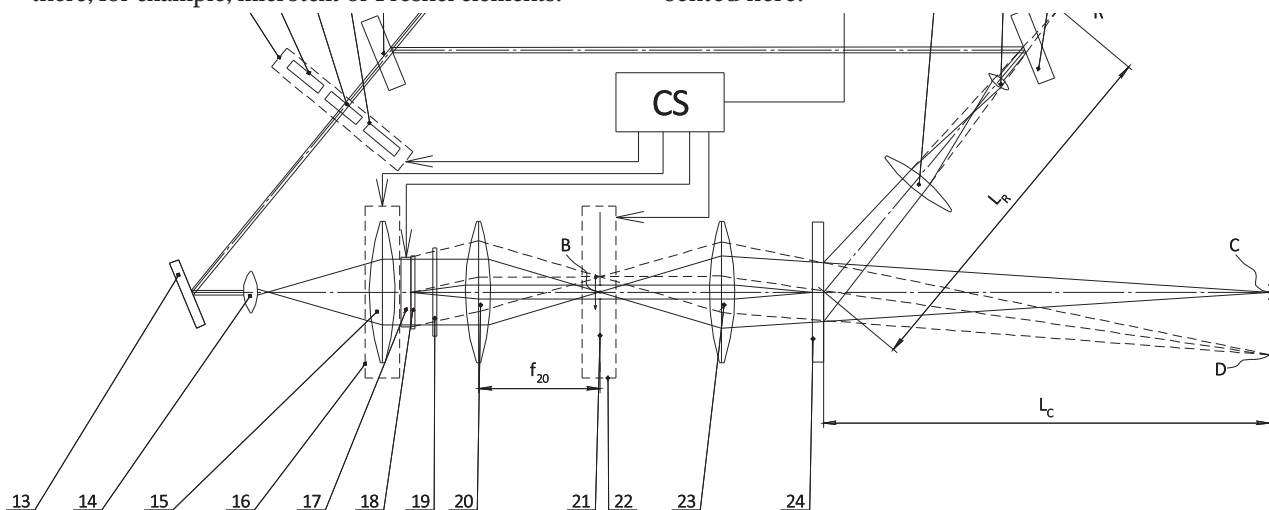


Fig. 7. Optical scheme for HS recording that implements one-step digital color HS formation with rasterless imaging in the hologram plane

The radiation of solid-state pulsed laser 1 (Geola RGB Alfa A1), which produces three separate beams of 440, 532 and 660 nm wavelengths, is combined into a single beam by the instrumental-

ity of a dichroic mirror 3–6 system. The laser consists of shutter assembly 2, opening for an exposition time and controlled from control system (CS), and half-wave plates in each beam trace, providing

necessary orientation of the polarization plane. In this set up, a vertical plane of the electric vector oscillations is adjusted. After the reflection with a mirror 7 by means of a semitransparent mirror 8, the combined radiation beam is divided into two: objective (OB) and reference (RB).

When exposed at stated wavelength, which is sequential, a corresponding half-wave plate 9, 10 or 11 aligns with the path of the OB, converting oscillations of the electric vector to the horizontal plane. That plates changeover is carried out in practice by displacement device 12, controlled from CS.

After a mirror 13 reflects OB, the telescopic arrangement with lenses 14 and 15 forms a collimated beam that supplies uniform illumination of the working window, constituting liquid crystal space-time light modulator (SLM) 17. The main functional part of the OB optical arrangement, including the elements 15–24 presented in Fig. 1, provides the sequential input by CS for the recorded images to SLM and then its projective transposition to the plane 24 of the recording medium by applying lenses 20 and 23.

A diffuser 18 is installed right behind SLM in direct contact. An analyzer 19 is located further along the light path passing the radiation with only vertical orientation of the electric vector and provides maximum contrast of the image observing beyond SLM. A stop 21 is installed in the back focal plane of the lens 20. Spatial-frequency spectrum (SFS) of radiation field behind SLM is formed in there. SFS with an extended scale has a complex structure due to the complex fine structure of SLM. The stop 21 cuts out the central informative part of the spectrum and by this means acts as a spatial filter.

In general, after the lens 23 forming the image on the recording medium the radiation beam converges at a point C situated at the stated distance after the recording medium. This distance corresponds to the one which is the observing distance while reconstructing the hologram. Considering given implementation of the apparatus this distance is $L_c = 400$ mm. In Fig. 7 solid lines represent ray path of OB, converging after the recording medium at the axis point C, when recording image at the central (axial) direction view. Ray path illustrates that the center of the beam separated by the stop 21 (point B) and the center of the beam, converging after the recording medium 23 (point C), are optically conjugated. The diffuser 18 provides the blurring of SFS central maximum within the

aperture of the stop 21 and, thereby, smooths out the intensity distribution in the convergence area of the OB after the recording medium.

The changeover of the images, entering to SLM, is accompanied with a transverse displacement of the lens 15 by applying the displacement mechanism 16. This provides direction change of the radiation beam, incident to LC SLM and lens 20, and, thereafter, the direction change of the radiation beam, forming the image in recording medium behind the lens 23. Due to the resulting SFS displacement in the focal plane of the lens 20 the corresponding shift of the filtering stop 21 is accomplished by displacement mechanism 22. This process is accompanied with the shift in the transverse direction of OB convergence point (from point C to point D). In Fig. 7 dashed lines represent ray path of the beams forming the image in the recording medium 24, when entering the certain image to SLM in accordance to the shift of the lens 15.

After reflected by the semitransparent mirror 8 laser radiation in the reference channel branch, is reflected by the mirror 25 towards the recording medium 24. RB, incident to the recording medium, is being transfigured into homocentric divergent beam by applying the lenses 26 and 27. Its divergence center R is arranged on a distance $L_r = 1$ m from the recording medium. This distance corresponds to the one, where reconstruction light source is situated when observing HS.

In considering implementation of the apparatus for the recording security HS, having relatively small dimensions (few cm) and being observed from the small distance ($L_c = 400$ mm as specified), the reconstructing light source is also situated at the small distance from the hologram. Here this distance is taken up as $L_c = 500$ mm. The incident angle of RB to the recording medium is about 45° .

During the single exposure, the resulting field of OB and RB interference is detected in photosensitive medium. The last one beam forms an object image in the certain direction of view by applying one of three stated wavelengths. The full cycle of the HS recording involves the sequential registration of the whole set of images for every wavelength, resulting the multiplexing HS. The whole set of OB points, converging after the recording medium, produce a virtual two-dimensional regular grating at some distance.

When observing the recorded HS the hologram itself, a reconstructed light source and an observ-

er are disposed in the same vertical plane. Given that, their relative position has to match to the relative position of the recording medium, the center R of the homocentric OB and the point C of RB convergence while recording HS, which in Fig. 7 are located in the figure plane. In the region of the observer's eyes locating the real image of aforementioned regular grating is reconstructed, wherefrom the parameter requirements for recording stage ensue. So this grating step have to not exceed the diameter of the observer's eye pupil (2–3 mm). The total size of the grating towards the connecting line of the observer's eyes (direction perpendicular to the plane of Fig. 7) has to far exceed the eye base size equal to 60 mm approximately. In the other direction, perpendicular to be written one, the grating size has to provide the stereo effect when shaking head in vertical plane.

With a considerable number of sequential exposures in the photosensitive material is equal to the product of the number of views for the recorded object by the number of color components this multiplexing. That always leads to substantial reduction in the diffraction efficiency in the reconstructed image, not only for certain direction of view or its color component, but also the entire HS. For some photosensitive media, for example, photopolymers, this exposure method of the photosensitive layer is not fundamentally suitable due to the formation and recording of the real interference pattern and the diffraction on that structure at every next exposures.

The considered set up optical scheme for the recording of full-parallax HS can also be applied for the recording of one-parallax HS, providing the effect of stereoscopic perception in one horizontal plane. In order to provide a sufficient vertical viewing angle for HS, the diffuser 18 has to have a broad scattering indicatrix in the appropriate direction coinciding with the figure plane, the stop 21 has to be a slit one.

As supplementary, the developed apparatus can be implemented as the alternate design for recording of the transparent HS. For that end, OB part of the apparatus, consisting of the elements 26, 27, has to be reversed symmetrically in the figure plane with the respect to the plane. This part forms a geometry of the beam in the region of the recording medium.

Fig. 8 represents the layout of image interchange and photographs of the reconstructed images of recorded color holographic stereograms when viewed from different angles.

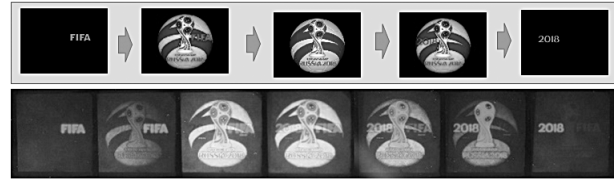


Fig. 8. Image interchange layout and photos of the reconstructed images of color HS

Conclusion

Angular and spectral selectivity, depending on incident angle of the reference beam, are defined. It is shown that the reflective holograms have 10–20 times higher spectral selectivity compared to transparent holograms, when incident angles of the reconstructed beam are over 40°. This provides the feasibility to observe clearer color in the image, reconstructed from the reflective hologram. Through the analysis, the method and apparatus for one-step color full-parallax holographic stereograms with a digital object and a rasterless image in hologram plane are developed. Samples of this type of hologram are recorded. The given single-stage set up scheme for HS enables to reduce the time of its recording by 2–3 times.

References

1. Gornostay AV, Odinkov SB. A method to design a diffractive laser beam splitter with color separation based on bichromated gelatine. *Computer Optics* 2016; 40(1): 45-50. DOI: 10.18287/2412-6179-2016-40-1-45-50.
2. Collier R, Burckhardt C, Lin L. *Optical Holography*. New York, London: Academic Press; 1971.
3. Kogelnik H. Coupled wave theory for thick hologram gratings. *The Bell System Technical Journal*, 1969; 48(9): 2909-2949. DOI: 10.1002/j.1538-7305.1969.tb01198.x.
4. Kihara N. Holographic stereogram forming apparatus. US Patent 7046409 B2, 16.05.2006.
5. Toyoda T, Kihara N, Shiracura A. Holographic stereogram printing system, holographic stereogram printing method and holographic device. US Patent 6559983, 06.05.2003.
6. Klug M, Holzbach M, Ferdman A. Method and apparatus for recording one-step, full-color, full-parallax, holographic stereograms. US Patent 6330088 B1, 11.12.2001.
7. Brotherton-Ratcliffe D, Vergnes FMR, Rodin A, Grichine M. Holographic printer. US Patent 6930811, 16.08.2005.
8. Brotherton-Ratcliffe D, Rodin A. Holographic printer. US Patent 7161722, 09.01.2007.

